



# Low-Rank Representation for Multi-center Autism Spectrum Disorder Identification

Mingliang Wang<sup>1</sup>, Daoqiang Zhang<sup>1(✉)</sup>, Jiashuang Huang<sup>1</sup>,  
Dinggang Shen<sup>2(✉)</sup>, and Mingxia Liu<sup>2(✉)</sup>

<sup>1</sup> College of Computer Science and Technology, Nanjing University of Aeronautics  
and Astronautics, Nanjing, China

[dqzhang@nuaa.edu.cn](mailto:dqzhang@nuaa.edu.cn)

<sup>2</sup> Department of Radiology and BRIC, University of North Carolina at Chapel Hill,  
Chapel Hill, NC, USA

[dgshen@med.unc.edu](mailto:dgshen@med.unc.edu), [mxliu@unc.edu](mailto:mxliu@unc.edu)

**Abstract.** Effective utilization of multi-center data for autism spectrum disorder (ASD) diagnosis recently has attracted increasing attention, since a large number of subjects from multiple centers are beneficial for investigating the pathological changes of ASD. To better utilize the multi-center data, various machine learning methods have been proposed. However, most previous studies do not consider the problem of data heterogeneity (*e.g.*, caused by different scanning parameters and subject populations) among multi-center datasets, which may degrade the diagnosis performance based on multi-center data. To address this issue, we propose a multi-center low-rank representation learning (MCLRR) method for ASD diagnosis, to seek a good representation of subjects from different centers. Specifically, we first choose one center as the target domain and the remaining centers as source domains. We then learn a domain-specific projection for each source domain to transform them into an intermediate representation space. To further suppress the heterogeneity among multiple centers, we disassemble the learned projection matrices into a shared part and a sparse unique part. With the shared matrix, we can project target domain to the common latent space, and linearly represent the source domain datasets using data in the transformed target domain. Based on the learned low-rank representation, we employ the k-nearest neighbor (KNN) algorithm to perform disease classification. Our method has been evaluated on the ABIDE database, and the superior classification results demonstrate the effectiveness of our proposed method as compared to other methods.

## 1 Introduction

Autism spectrum disorder (ASD) is associated with a range of phenotypes, such as poor social communication abilities, repetitive patterns of behavior, and

---

This study was supported by National Natural Science Foundation of China under Grant 61876082, 61861130366, 61703301, and 61473149.

restricted interest. It was reported that there were 62.2 million ASD cases in the world in 2015 [1]. However, the pathological mechanism of ASD is unclear, and conventional diagnosis of ASD is usually based on symptoms [2], and thus the precise diagnosis is the main challenge in the research literature of ASD.

Neuroimaging is a powerful tool for characterizing neural patterns of functional connectivity using resting-state functional magnetic resonance imaging (rs-fMRI) data, and has been widely applied to ASD diagnosis. Recently, multi-center rs-fMRI datasets are available for studying of ASD disease and many researchers have devoted their efforts to take advantage of increasing amounts of multi-center data. Existing methods [3–5] either try to diagnose ASD using data from each imaging center separately, or straightforwardly combine multi-center datasets for disease analysis. However, these methods do not consider the facts that there is usually a limited number of imaging data at each center and datasets from different centers often have heterogeneous characteristics. Recently, low-rank representation (LRR) [6] has been successfully applied to neuroimage-based brain disease analysis, which helps uncover the underlying structure of data by suppressing noisy features. For example, Adeli *et al.* [7] developed a joint feature-sample selection method to diagnose Parkinson’s disease with a low-rank constraint. Vounou *et al.* [8] proposed a sparse reduced-rank regression model to identify potential genetic data associated with Alzheimer’s disease. However, these studies generally ignore the problem of data heterogeneity (*e.g.*, caused by different scanning parameters and subject populations) among different centers, thus leading to sub-optimal performance.

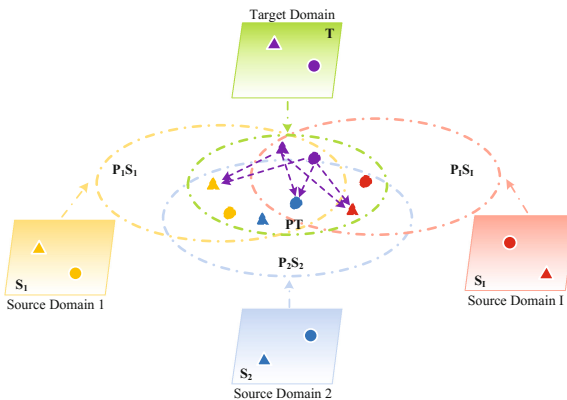


**Fig. 1.** Illustration of our multi-center low-rank representation learning method. There are  $I$  source domains and a target domain. Each source domain (denoted as  $\mathbf{S}_i$ ) and the target domain (denoted as  $\mathbf{T}$ ) contain two samples (marked as triangles and circles) belonging to two categories. Our method transforms each source domain  $\mathbf{S}_i$  into an intermediate representation  $\mathbf{P}_i\mathbf{S}_i$ , and each transformed sample can be linearly represented by the target samples with a common latent projection (*i.e.*,  $\mathbf{PT}$ ).

Accordingly, in this paper, we propose a novel unsupervised multi-center low-rank representation (MCLRR) learning method to learn the latent representation of multi-center data for ASD disease diagnosis. The framework of our proposed method is described in Fig. 1. As illustrated in Fig. 1, we treat the center that needs to be analyzed as target domain and the remaining centers as source domains. In addition, we also assume that no label information is available for samples in the target domain, while samples in source domains are well labeled. Then we transform each source domain into an intermediate latent representation space, such that each transformed sample can be linearly represented by samples in the target domain. As a result, the heterogeneity across different centers can be partly alleviated. To further reduce the heterogeneity of different centers, we disassemble each learned projection matrix of source domains into a shared projection matrix and a space unique matrix. And the target domain can be transformed into the latent space using the learned shared projection. With the transformed target domain dataset, we can well represent the source domain datasets. Finally, we employ the k-nearest neighbor (KNN) algorithm on the latent space by using the labeled source domain datasets to arrive a final classification decision of the target domain.

## 2 Method

**Data and Pre-processing:** In this study, we use rs-fMRI data from the Autism Imaging Data Exchange (ABIDE) database<sup>1</sup>, a large multi-center autism dataset. It contains a total of 871 quality rs-fMRI data from 17 different centers. Due to the limited number of participants in several centers, we select 468 subjects from 5 different centers (with the number of subjects >50), including *Leuven*, *NYU*, *UCLA*, *UM* and *USM*. Specifically, there are 250 ASD patients and 218 normal controls (NCs), and the numbers of patients and NCs in each center are comparable.

We download the pre-processed rs-fMRI data with the Configurable Pipeline for the Analysis of Connectomes (C-PAC) from the Preprocessed Connectome Project<sup>2</sup>. The image pre-processing steps include slice timing corrected, motion correction, and normalization of the intensity. Subsequently, the signal fluctuations induced by head motion, respiration, cardiac pulsation, and scanner drift were removed by conducting the nuisance regression. Afterward, the anatomical automatic labeling (AAL) atlas with 116 pre-defined regions-of-interest (ROIs) was aligned onto each image, followed by extracting ROI-based mean time series for each subject. Finally, based on the pairwise Pearson correlation coefficients, a functional connectivity matrix was conducted, where each edge weight is the correlation between a pair of ROIs. For simplicity, the upper triangle (symmetric with lower triangle) and the diagonal values (*i.e.*, correlation of an ROI to itself) of the matrix were removed, and the remaining triangles were converted

---

<sup>1</sup> [http://fcon\\_1000.projects.nitrc.org/indi/abide/](http://fcon_1000.projects.nitrc.org/indi/abide/).

<sup>2</sup> <http://preprocessed-connectomes-project.org>.

to a vector as the features. Thus, we obtained a 6,670 dimensional feature vector for representing each subject.

**Multi-center Low-Rank Representation:** In this study, we formulate the multi-center ASD diagnosis as a low-rank representation based classification problem, where one center is chosen as the target domain and the remaining centers as source domains. Suppose there are  $I$  source domains, each source domain is composed of a set of  $N_i$  subjects  $\mathbf{S}_i = [\mathbf{s}_1, \dots, \mathbf{s}_{N_i}] \in \mathbb{R}^{d \times N_i}$ , and a set of  $N_T$  subjects  $\mathbf{T} = [\mathbf{t}_1, \dots, \mathbf{t}_{N_T}] \in \mathbb{R}^{d \times N_T}$  in the target domain, where  $d$  is the dimension of the feature vector. Our aim is to find an intermediate latent space, via the low-rank transformation matrix  $\mathbf{P}_i$  to represent source domains using the target domain. The proposed objective function is defined as:

$$\begin{aligned} & \min_{\mathbf{P}_i, \mathbf{Z}_i, \mathbf{E}_i^Z} \sum_{i=1}^I (\text{rank}(\mathbf{Z}_i) + \alpha \|\mathbf{E}_i^Z\|_1) \\ & \text{s.t. } \mathbf{P}_i \mathbf{S}_i = \mathbf{T} \mathbf{Z}_i + \mathbf{E}_i^Z, i = 1, \dots, I \end{aligned} \quad (1)$$

where  $\text{rank}(\mathbf{Z}_i)$  is the rank of matrix  $\mathbf{Z}_i$ ,  $\|\mathbf{E}_i^Z\|_1 = \sum_{j=1}^{N_i} \sum_{i=1}^d |\mathbf{E}_{i,j}^Z|$  is  $\ell_1$ -norm, and  $\alpha$  is a parameter to balance the contributions of low-rank constraint and sparse regularization. Although it is difficult to solve the rank minimization in Eq. (1) directly, *nuclear norm* provides a good surrogate for addressing it. Therefore, the Eq. (1) can be rewritten as:

$$\begin{aligned} & \min_{\mathbf{P}_i, \mathbf{Z}_i, \mathbf{E}_i^Z} \sum_{i=1}^I (\|\mathbf{Z}_i\|_* + \alpha \|\mathbf{E}_i^Z\|_1) \\ & \text{s.t. } \mathbf{P}_i \mathbf{S}_i = \mathbf{T} \mathbf{Z}_i + \mathbf{E}_i^Z, i = 1, \dots, I \end{aligned} \quad (2)$$

where  $\|\cdot\|_*$  denotes the nuclear norm of a matrix, which can be calculated by the sum of singular values of the matrix.

It is worth noting that it could be sub-optimal to reconstruct data from source domain in the original target domain, since data acquired from different centers are usually heterogeneous. Since the underlying pathology of ASD disease among multiple centers is the same, it is intuitive to assume that multiple centers share an intrinsic latent representation space. Accordingly, we can disassemble the transformation matrix  $\mathbf{P}_i$  into a shared latent space via both a low-rank matrix  $\mathbf{P}$  and a unique sparse matrix  $\mathbf{E}_i^P$  for the  $i$ -th source domain. By transforming the target domain to the latent space with the matrix  $\mathbf{P}$ , our multi-center low-rank representation (MCLRR) learning method can be described as:

$$\begin{aligned} & \min_{\mathbf{P}, \mathbf{P}_i, \mathbf{Z}_i, \mathbf{E}_i^Z, \mathbf{E}_i^P} \|\mathbf{P}\|_* + \sum_{i=1}^I (\|\mathbf{Z}_i\|_* + \alpha \|\mathbf{E}_i^Z\|_1 + \beta \|\mathbf{E}_i^P\|_1) \\ & \text{s.t. } \mathbf{P}_i \mathbf{S}_i = \mathbf{P} \mathbf{T} \mathbf{Z}_i + \mathbf{E}_i^Z, \\ & \mathbf{P}_i = \mathbf{P} + \mathbf{E}_i^P, i = 1, \dots, I \\ & \mathbf{P} \mathbf{P}^T = \mathbf{I} \end{aligned} \quad (3)$$

where  $\beta$  is the balanced parameter between shared and variance part, and the orthogonal constraint  $\mathbf{P}\mathbf{P}^T = \mathbf{I}$  is imposed to avoid trivial solutions of matrix  $\mathbf{P}$ . In Eq. (3), the common low-rank matrix  $\mathbf{P}$  can uncover most of the shared information amongst multi-center ASD datasets. The rank of matrix  $\mathbf{E}_i^Z$  tends to find a representation coefficient on the transformed target domain space. The minimization of  $\|\mathbf{E}_i^Z\|_1$  and  $\|\mathbf{E}_i^P\|_1$  encourages the error of reconstruction matrix and variance matrix to be sparse.

**Optimization:** The problem in Eq. (3) is a typical mixed nuclear norm and  $\ell_1$ -norm minimization optimization. In this paper, we adopt the Augmented Lagrange Multiplier (ALM) to solve the objective function. We first transform Eq. (3) into the following equivalent formulation:

$$\begin{aligned} & \min_{\mathbf{J}, \mathbf{P}, \mathbf{P}_i, \mathbf{Z}_i, \mathbf{E}_i^Z, \mathbf{E}_i^P, \mathbf{F}_i} \quad \|\mathbf{J}\|_* + \sum_{i=1}^I (\|\mathbf{F}_i\|_* + \alpha\|\mathbf{E}_i^Z\|_1 + \beta\|\mathbf{E}_i^P\|_1) \\ & \text{s.t. } \mathbf{P}_i \mathbf{S}_i = \mathbf{P} \mathbf{T} \mathbf{Z}_i + \mathbf{E}_i^Z, \\ & \quad \mathbf{P}_i = \mathbf{P} + \mathbf{E}_i^P, i = 1, \dots, I \\ & \quad \mathbf{P} \mathbf{P}^T = \mathbf{I}, \mathbf{P} = \mathbf{J}, \mathbf{Z}_i = \mathbf{F}_i \end{aligned} \quad (4)$$

Then the augmented Lagrange function can be defined as follows:

$$\begin{aligned} & \min_{\mathbf{J}, \mathbf{P}, \mathbf{P}_i, \mathbf{Z}_i, \mathbf{E}_i^Z, \mathbf{E}_i^P, \mathbf{F}_i, \mathbf{Y}_{1,i}, \mathbf{Y}_{2,i}, \mathbf{Y}_{3,i}, \mathbf{Y}_4} \quad \|\mathbf{J}\|_* + \sum_{i=1}^I (\|\mathbf{F}_i\|_* + \alpha\|\mathbf{E}_i^Z\|_1 + \beta\|\mathbf{E}_i^P\|_1 + \frac{\mu}{2}\|\mathbf{P}_i \mathbf{S}_i - \mathbf{PTZ}_i - \mathbf{E}_i^Z\|_F^2 + \frac{\mu}{2}\|\mathbf{P}_i - \mathbf{P} - \mathbf{E}_i^P\|_F^2 + \frac{\mu}{2}\|\mathbf{Z}_i - \mathbf{F}_i\|_F^2 + \\ & \quad \langle \mathbf{Y}_{1,i}, \mathbf{P}_i \mathbf{S}_i - \mathbf{PTZ}_i - \mathbf{E}_i^Z \rangle + \langle \mathbf{Y}_{2,i}, \mathbf{P}_i - \mathbf{P} - \mathbf{E}_i^P \rangle + \\ & \quad \langle \mathbf{Y}_{3,i}, \mathbf{Z}_i - \mathbf{F}_i \rangle) + \langle \mathbf{Y}_4, \mathbf{P} - \mathbf{J} \rangle + \frac{\mu}{2}\|\mathbf{P} - \mathbf{J}\|_F^2 \end{aligned} \quad (5)$$

where  $\langle \cdot, \cdot \rangle$  denotes the inner product of two matrices, *i.e.*,  $\langle \mathbf{A}, \mathbf{B} \rangle = \text{tr}(\mathbf{A}^T \mathbf{B})$ .  $\mathbf{Y}_1, \mathbf{Y}_2, \mathbf{Y}_3$  and  $\mathbf{Y}_4$  are Lagrange multipliers and  $\mu > 0$  is a penalty parameter.

While it is difficult to jointly update the variables in Eq. (5), we can still optimize each of them in the leave-one-out fashion. Hence, we alternately optimize each variable iteratively with fixed values of the others and resort to ALM to solve the objective function. Once we obtain the representation of transformed target domain (*i.e.*,  $\mathbf{PT}$ ) and source domains (*i.e.*,  $\mathbf{PTZ}_i$ ), we can use the KNN algorithm to estimate the final label of a test sample.

### 3 Experiments

**Experimental Settings:** We evaluated the proposed MCLRR method in ASD vs. NC classification based on multi-center data from the ABIDE database.

The performance was measured via four criteria, *i.e.*, classification accuracy (ACC), sensitivity (SEN), specificity (SPE) and area under the ROC curve (AUC).

We first compared our MCLRR method with 3 baseline methods, including KNN, support vector machine (SVM), and classical low-rank representation (LRR) method [6]. To investigate the influence of our learned latent representation, we further compare MCLRR with its variant (denoted as MCLRR-1) without mapping data of target domain to the latent space. That is, MCLRR-1 directly employ data in the original target domain to represent data in source domains (without learning the shared transform matrix), while MCLRR transforms the target domain to a shared space for representing multiple source domains. Different from KNN and SVM methods that use the original rs-fMRI features for classification, LRR and our methods (*i.e.*, MCLRR-1 and MCLRR) first learn new representations of data and then feed the new features into a 5-nearest neighbor classifier for disease classification. Besides, we compare MCLRR with 3 state-of-the-art methods for ASD diagnosis, including a graph-based convolutional network [3] with hinge loss (denoted as sGCN-1) and global loss (denoted as sGCN-2), functional connectivity association analysis with leave-one-out classifier (FCA) [4], and a denoising autoencoder (DAE) [5] with two autoencoders.

In the experiments, we select one from multiple centers in turn as the target domain and regard the remaining ones as source domains. A 5-fold cross-validation (CV) strategy was used for performance evaluation. Specifically, the subjects of each domain are randomly partitioned into 5 subsets, and the subjects within one subset are selected as the test data each time, while all other subjects in the remaining subsets are used to train the models. To obtain the optimal parameters in different methods, we further performed a 5-fold inner CV using training data. The parameters in MCLRR-1 (*i.e.*,  $\alpha$ ) and MCLRR (*i.e.*,  $\alpha$  and  $\beta$ ) are chosen from  $\{1e^{-3}, \dots, 1e^3\}$ , respectively. The parameter  $\lambda$  in LRR was also set to  $\{1e^{-3}, \dots, 1e^3\}$  to balance the low-rank constraint and the outliers detection. For SVM method, we use the linear SVM classifier with parameters (*i.e.*,  $C$ ) selected from the range of  $\{2^{-5}, \dots, 2^5\}$ . The parameter  $k$  for the KNN method was chosen from  $\{3, 5, 7, 9, 11, 15\}$ .

**Results:** We report the experimental results achieved by our method and those baseline methods in Fig. 2. As can be seen from Fig. 2, we can derive several interesting observations. *First*, low-rank-based methods (*i.e.*, LRR, MCLRR-1, and MCLRR) generally achieve better performance in most cases. For example, the average ACC values (*i.e.*, across multiple centers) achieved by low-rank-based methods are 63.92%, 63.60% and 68.74% respectively, which are noticeably higher than those of KNN and SVM methods (*i.e.*, 58.71% and 61.02%). This demonstrates that low-rank-based representation is useful in dealing with the problem of data heterogeneity by discovering the underlying data structure among different imaging centers. *In addition*, our proposed MCLRR method consistently outperforms MCLRR-1 in terms of ACC, SEN and AUC on

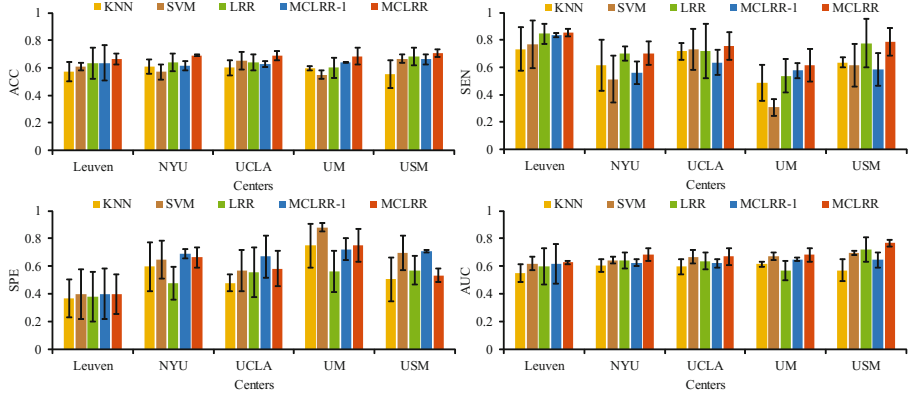


**Fig. 2.** Performance of proposed MCLRR method and three baseline methods in ASD vs. NC classification using multiple centers data.

multiple centers datasets. These results validate the efficacy of our proposed strategy that projects multi-center data into an intermediate latent representation space.

We further report the comparison between our method and state-of-the-art methods for ASD identification on the *NYU* center in Table 1. It can be seen from Table 1 that our MCLRR method achieves higher accuracy (*i.e.*, 69.10%), specificity (*i.e.*, 66.43%) and AUC (*i.e.*, 68.33%) than 4 competing methods, even though sGCN and DAE are two deep-learning methods.

**Table 1.** Comparison with state-of-the-art methods for ASD identification using rs-fMRI ABIDE data. FNC: Functional Network Connectivity; KNN: k-nearest neighbor algorithm.

Methods	Feature type	Classifier	ACC (%)	SEN (%)	SPE (%)	AUC (%)
sGCN-1 [3]	FNC	KNN	60.50	–	–	57.00
sGCN-2 [3]	FNC	KNN	63.50	–	–	61.00
FCA [4]	FNC	<i>t</i> -test	63.00	72.00	58.00	–
DAE [5]	FNC	Softmax regression	66.00	66.00	65.00	–
MCLRR (ours)	FNC	KNN	<b>69.10</b>	70.24	<b>66.43</b>	<b>68.33</b>

## 4 Conclusion

We present a novel low-rank representation method using multi-center data for ASD diagnosis. Specifically, to alleviate the heterogeneities of multi-center datasets, we first learn the projection matrices to transform the source domains into a latent representation space. Also, we disassemble the learned projection

matrix into a shared matrix and a sparse matrix. Then, we transform the target domain into the latent space with the shared projection matrix, and linearly represent the source domain datasets using data in the transformed target domain. A k-nearest neighbor method is employed to arrive at a final classification decision. Results on the ABIDE database demonstrate the effectiveness of our method in ASD diagnosis using rs-fMRI data acquired from multiple centers. In the future, we will perform data-driven feature extraction for rs-fMRI data via deep learning [9–11] rather than using current hand-crafted (*i.e.*, ROI) features, which is expected to further improve the diagnostic performance.

## References

1. Catal-Lpez, F., et al.: Risk of mortality among children, adolescents, and adults with autism spectrum disorder or attention deficit hyperactivity disorder and their first-degree relatives: a protocol for a systematic review and meta-analysis of observational studies. *Syst. Rev.* **6**(1), 189 (2017)
2. Wang, J., et al.: Multi-task diagnosis for autism spectrum disorders using multi-modality features: a multi-center study. *Hum. Brain Mapp.* **38**(6), 3081–3097 (2017)
3. Ktena, S.I., et al.: Metric learning with spectral graph convolutions on brain connectivity networks. *Neuroimage* **169**, 431–442 (2017)
4. Nielsen, J.A., et al.: Multisite functional connectivity MRI classification of autism: ABIDE results. *Front. Hum. Neurosci.* **7**(599), 1–12 (2013)
5. Heinsfeld, A.S., Franco, A.R., Craddock, R.C., Buchweitz, A., Meneguzzi, F.: Identification of autism spectrum disorder using deep learning and the ABIDE dataset. *Neuroimage Clin.* **17**, 16–23 (2017)
6. Liu, G., Lin, Z., Yu, Y.: Robust subspace segmentation by low-rank representation. In: Proceedings of the 27th International Conference on Machine Learning, ICML 2010, Haifa, pp. 663–670 (2010)
7. Adeli, E., et al.: Joint feature-sample selection and robust diagnosis of Parkinson’s disease from MRI data. *Neuroimage* **141**, 206–219 (2016)
8. Vounou, M., et al.: Sparse reduced-rank regression detects genetic associations with voxel-wise longitudinal phenotypes in Alzheimer’s disease. *Neuroimage* **60**(1), 700–16 (2012)
9. Liu, M., Zhang, J., Adeli, E., Shen, D.: Landmark-based deep multi-instance learning for brain disease diagnosis. *Med. Image Anal.* **43**, 157–168 (2018)
10. Lian, C., et al.: Multi-channel multi-scale fully convolutional network for 3D perivascular spaces segmentation in 7T MR images. *Med. Image Anal.* **46**, 106–117 (2018)
11. Zhang, J., Liu, M., Shen, D.: Detecting anatomical landmarks from limited medical imaging data using two-stage task-oriented deep neural networks. *IEEE Trans. Image Process.* **26**(10), 4753–4764 (2017)